



Customization of residual stress induced in cold spray printing

Bahareh Marzbanrad, Ehsan Toyserkani, Hamid Jahed *

Mechanical and Mechatronics Engineering Department, University of Waterloo, Canada

ARTICLE INFO

Associate Editor: Yip-Wah Chung

Keywords:

Cold spray
Residual stress
Thermal effects
Mechanical strain
Aluminum
Magnesium

ABSTRACT

It is generally believed that because of deposition at a temperature lower than the melting point, and high impact velocity of particles in cold spray printing, beneficial compressive residual stresses are induced in the substrate and coating. We have examined this general belief by identifying four major factors influencing the formation of residual stresses: coating and impact-induced temperatures, thermal mismatch of coat and substrate, heat transfer rate, and impact peening effect. A series of experiments is developed to allow studying these effects separately and to investigate their interactions. It is concluded that the heat input and heat transfer rate are the key controlling factors in the sign of the residual stress. Furthermore, we show that one can control the formation of residual stress to a desirable pattern, i.e., compressive in both the coating and the substrate near the interface. Using such parameters, two distinct residual stresses, tensile and compressive, were produced in the Al7075 coated AZ31B sheet. Further, the quality of the two coatings is measured through computerized tomography, surface roughness, and hardness measurements. It is shown that the density and hardness of the compressive samples are higher, while the roughness is lower than the tensile sample.

1. Introduction

Coating formation in solid-state is materialized through the promising cold gas spraying process whereby micron-size particles are accelerated to a supersonic velocity (300–1200 m/s) towards the substrate by a pressurized and relatively-low-temperature carrier gas through a de Laval nozzle. Mechanical and metallurgical bonding with the substrate is produced by intensive plastic deformation and the localized heat generation upon impact resulting from the high kinetic energy of particles, as stated by Assadi et al. (2003). This solid-state bonding mechanism, which occurs as a result of the lower process temperature (much less than the particles' melting point) and the higher velocity of particles, makes it distinctive from other types of thermal spray coating processes. Continuous bombarding of the substrate with high-velocity particles generates high local strain in the coating and in the vicinity of the interface and contributes to the development of compressive residual stress in the coating and substrate. However, it has been reported in the literature, such as (Sampath et al., 2004) that the induced residual stress in coated materials is influenced by thermal features, including, but not limited to, the temperature gradient, cooling rate, and thermal mismatch in dissimilar coatings. These factors have the capability of relieving the stress or converting it from the expected compressive stress to tensile stress, depending on the coating and

substrate materials involved and the processing parameters. Since the residual stress might have destructive effects on the integrity of the coating, adhesion strength, peeling, and delamination, it should be carefully assessed in order to enhance the coating performance. Additionally, as reported by (Diab et al., 2017), the coated material with destructive residual stresses can be susceptible to early fatigue crack initiation, reducing the fatigue life of the coated part. Therefore, it is imperative to evaluate the residual stress of cold spray coated samples, both in the coating and substrate parts.

To the best of our knowledge, only a limited number of studies have explored the residual stress distribution developed by cold spraying. Matejicek and Sampath (2001) used the micro-diffraction approach to measure the residual stress in cold-sprayed copper particles. Compressive residual stresses were observed in all coated samples, despite the use of different particle velocities. They concluded that even though particle velocity significantly affects deposition efficiency, it has no effect on the residual stress development in cold-sprayed splats. Song et al. (2018) employed numerical simulation and direct measurement technique (Focused Ion Beam-Digital Image Correlation) to measure and evaluate the micro-residual stress in a single particle. They identified a correlation between compressive residual stress at the interface with the impact velocity for Ti-6Al-4 V particles. Luzin et al. (2011) measured the residual stress on Al/Cu coating and substrate materials using the

* Corresponding author.

E-mail address: hamid.jahed@uwaterloo.ca (H. Jahed).

neutron diffraction method and then compared the results with those from Tsui and Clyne's progressive model (Tsui and Clyne, 1997). They concluded that the residual stress was affected by plastic deformation, the kinetic parameters of the coating process, and the coating material properties, while the thermal effects were neglected. Recently, Wang et al. (2020) confirmed similar results through numerical simulation and experimental observations. They coated copper substrate with copper microparticles. Based on their results, the impact of the microparticles, the interactions between microparticles in the same layer, and interactions between microparticles in different layers are the most affecting parameters on residual stress. They did not consider thermal effects in their studies. However, Araghi et al. (2014) found that the thermal input and corresponding thermal history had a significant effect on the residual stress profile when they coated copper on copper and steel substrates. They measured the temperature changes and distortion by a thermocouple and Almen gauge, respectively. They concluded that the type of coating and substrate materials, as well as their geometry, have a major influence on the sign and magnitude of the distortion, which can change the residual stress distribution. In another study, Suhonen et al. (2013) investigated the role of different material combinations—Al, Cu, and Ti coatings and carbon steel, stainless steel, and aluminum substrate materials—on residual stress formation. Using a curvature-based approach to determine the deflection of the coated materials during coating deposition, they measured the residual stress. Based on their results, they observed that pretreatment of a substrate (grit blasting) as well as the features of coating and substrate materials, can shift the residual stress arising with cold spraying from compressive to neutral and tensile stresses. In another research, Sova et al. (2017) studied the effect of turning and ball burnishing post-treatments on the residual stress of cold spray samples, in which 17–4PH stainless steel was deposited on the AA1050 substrate. The reported results showed that the compressive residual stress at the coating surface of as-sprayed samples was converted to the tensile after machining (turning) and then turned back to the compressive when the turned samples were further finished by ball burnishing. Boruah et al. (2019) evaluated the residual stresses induced by cold spraying of Ti-6Al-4 V on a Ti-6Al-4 V substrate. They employed neutron diffraction and contour methods to measure the residual stress through the depth and investigated the effect of the number of cold spray layers, the thickness of the substrate and coating, and the track pattern on the magnitude and distribution of residual stress in the coated samples. Based on the result of this research, the magnitudes of the residual stress were found to be dependent on the geometrical values, but all had the same trend. The maximum compressive residual stress was induced at the interface, while the high tensile residual stress was formed near the free surface of the Ti-64 coating and towards the bottom of the substrate. They concluded that rising temperature and a fast cooling rate were the main factors affecting residual stress distribution rather than the peening effect. However, Singh et al. (2018) claimed that the compressive residual stress, induced in the cold sprayed IN 718 coatings, is strongly influenced by the peening effect even though the thickness of a coating can also affect the magnitude of the compressive residual stress. In another study, Ghelichi et al. (2012) coated Al5052 substrates with pure Al and Al7075 to investigate the role of coating materials and deposition parameters on the fatigue life of the coated samples. They showed that coating materials and processing parameters have strong effects on the fatigue strength improvement of the substrate materials, whereas compressive residual stress can be observed in all sets of experiments independent of the coating parameters and materials. Shayegan et al. (2014) studied the impact of aluminum particles on AZ31B by developing a thermo-mechanical model in LS-Dyna. Different cold spray parameters, including particle shape, size, velocity, incident angle, friction, and their effects on the residual stress were studied. They concluded that particle speed changes the depth of the compressive residual stress zone, but particle size and shape have little to no effect. In recent work, Marzbanrad et al. (2018) coated Al7075 on AZ31B magnesium alloy sheets

and measured the residual stress of the coated samples under different deposition parameters. In this research, the strain evolution during the cold spray process was monitored with embedded fiber Bragg grating sensors. The results revealed that the development of compressive residual stress in Mg coated samples is strongly influenced by thermal energy as a predominant factor, rather than the peening effect; hence, the residual stress could be released or restored as tensile stress in the temperature-sensitive substrate materials. Considering the possible harmful effects of tensile residual stress and the mechanical performance of the cold spray coated Mg substrates, optimizing the deposition parameters seems necessary to sustain the beneficial residual stress in coated parts.

In this research, AZ31B magnesium alloy, the lightest commercially available metal with a high strength to weight ratio, is considered as a substrate material on which Al7075 aluminum powder is deposited. Because of the great interest in using Mg alloys for light-weighting in the automotive and aerospace industries, even though AZ31B has shown promising fatigue strength as demonstrated by (Toscano et al., 2017), it would be valuable to more improve its fatigue performance by employing cold spray (Dayani et al., 2018). To do so, surface treatment with a cold spray process is carried out to induce beneficial residual stresses. The effect of thermal mismatch on the residual stress of the Al7075/AZ31B samples is simulated. The influence of substrate temperature on the final residual stress formation of the coated parts is also investigated. An in-situ substrate temperature measurement using embedded thermocouple allowed studying the role of different heat transfer scenarios on resulting stresses. An attempt was then made to customize the residual stress pattern to a desirable condition by choosing coating parameters that accelerate heat transfer or minimize the heat input. Finally, the quality of coating, such as coating defects, coating thickness, surface roughness, and hardness, is examined under the various processing parameters and conditions.

2. Experimental procedure

2.1. Materials and methodology

In this study, a 3.16 mm thick AZ31B-H24 magnesium alloy sheet was cut into several 30 × 50 mm rectangular coupons as the substrate samples. Heat treatment (260 °C/15 min) (Metal Handbook: 4E: Heat Treating of Nonferrous Alloys, 2018) was carried out on the as-received samples based on the ASM-recommended procedure to ensure the identical mechanical state for all specimens. Before spraying, the substrate surface was polished using 1200 SiC grit paper and cleaned with ethanol. The feedstock powder used in the experiments was a spherical-shaped commercial Al7075 powder supplied by Centerline Ltd., Windsor, Canada, with an average value of 23 µm measured by Retsch technology, Camsizer XT (Marzbanrad et al., 2018). Table 1 lists the chemical compositions of AZ31B-H24 (Behravesh et al., 2011) and Al7075 powder. A 300 µm diameter hole was drilled parallel to the surface for embedding a thermocouple where it could be accommodated 100 µm from the substrate surface in the middle of the coating zone. After the thermocouple was embedded in the hole, it was fixed in place with a thin layer of thermal epoxy 353ND EPO-TEK cured at 150 °C (TECHNOLOGY, 2014). The low-pressure cold spray system used for conducting these experiments was a commercial Supersonic Spray Technologies (SST) Series P Cold Spray System (Centerline, Windsor, Canada). The propellant gas was nitrogen (N₂) streamed at the low pressure of 1.38 MPa.

The cold spray processing parameters that were used for depositing Al7075 on the Mg alloy substrates are shown in Table 2. The coating parameters were kept constant for all experiments except for the feed rate and nozzle speed. The main characteristics of cold spray coating, including mechanical and thermal properties, are known to intensely affect the residual stress. The mechanical effects introduced by peening and thermal effect are divided into thermal mismatch and coating

Table 1

Chemical composition of AZ31B-H24 (Xue et al., 2019) and Al7075 coating.

Composition (Weight %)	Aluminum (Al)	Zinc (Zn)	Manganese (Mn)	Iron (Fe)	Nickel (Ni)	Silicon (Si)	Copper (Cu)	Chromium (Cr)	Magnesium (Mg)	Other Elements
AZ31B-H24	2.99	0.95	0.2	0.005	–	0.05	0.05	–	Bal.	–
Al7075	90	5.20	–	0.35	0.005	–	1.55	0.25	2.35	0.30

Table 2

Cold spray coating parameters.

Carrier Gas			Nozzle					Studied Variables		
Type	Temperature	Pressure	Type	Length	Orifice Diameter	Exit Diameter	Stand-off Distance	Powder Feed Rate	Nozzle Speed	Step Over
N ₂	400 °C	1.38 MPa	De Laval UltiLife™	120 mm	2 mm	6.3 mm	12 mm	25% (8 g/min), 50% (16 g/min)	2, 5, 10, 20 mm/s	1.2 mm

temperature, including carrier gas temperature and deformation temperature. The role of thermal mismatch has been studied by a simple simulation to assess the influence of the material properties and coating geometries. However, the effect of coating temperature and peening effect can be evaluated by changing the most effective processing parameters such as feed rate and nozzle speed. Based on these parameters, several experiments have been designed to study the residual stress formation in the coating and substrate. Then in two extreme situations, where the tensile and compressive residual stress can be developed in the sample (which are named “tensile sample” and “compressive sample”), the quality of the coating and characteristics of the deposited material, including surface roughness and hardness are investigated.

2.2. Residual stress measurement

Residual stresses were measured using a Sint Technology hole drilling device, Restan MTS-3000. With the help of Fras-2 strain rosettes surface and through the depth, residual stresses were obtained in the coated samples. Before installing the strain gauges, the coated surface was polished to reduce surface roughness and increase the bonding strength between the strain gauges and the coating surface. This surface treatment reduces the thickness of the coating by at most 20 µm. During drilling, strain relief was measured incrementally through the strain gauge rosettes in three different directions. Then, the ASTM E837–13 (non-uniform stress field) method (Schajer, 1988) with the Tikhonov regularization algorithm was employed to calculate the residual stress up to 1 mm through the depth of the coated structure.

2.3. Surface roughness and hardness measurements

Surface roughness (Sa) for all coated samples was measured using a Keyence VK-X250 confocal laser microscope manufactured by Keyence Corporation, Osaka, Japan. The scanning areas for the surfaces of all coated samples had the same dimensions of 4 × 6 mm. The coating's thickness was measured using the Keyence microscope with 0.5 µm precision. In addition, Vickers microhardness testing was performed on cross-sectioned of the various coated samples with different processing parameters by using Clemex Technologies (Inc, Longueuil, Canada). Several indentations with a 50 g load were applied on the polished intersection in three different regions of the samples: the coating, interface, and substrate.

2.4. Tomography of the coating

A non-destructive method, X-ray computerized micro-scale tomography (CT) scanning, was performed using a ZEISS Xradia 520 Versa 3D X-ray microscope (ZEISS, Oberkochen, Germany) to study and compare the integrity of the coating when different processing parameters were

used (Salarian and Toyserkani, 2018). A volume with dimensions of 5.6 × 4.7 × 3.26 mm was specified for the scanning to identify the distribution of pores/defects close to the surface of the coated samples. A total of 2001 2D projections were recorded, with a voxel size of 3.5 µm for each sample. Table 3 lists the parameters used for the CT scan. After scanning, for image processing and analysis of the pores sizes and distributions, 2D projections were recreated using Dragonfly Pro v3.1 software (Object Research Systems (ORS), Montreal, Canada).

2.5. Numerical simulation

Thermal stress development in the cold spray coated sample was simulated by a two-dimensional numerical isotropic and linear elastic finite element models coupled with a heat transfer model using COMSOL Multiphysics software. The deformation was assumed to have a generalized plane strain condition. The coefficients of thermal expansions are assumed to be constant at different temperatures. The temperature of the plates is considered to be homogenous. To avoid any external stress on the plates, only the bottom left corner of the simulation domain was fixed. In each step, the temperature was adjusted to its determined temperature. In this simulation, the system was meshed by using the square adoptive meshing of COMSOL Multiphysics. This model consists of three layers: 1) Al7075 coating as a top layer with variable thicknesses between 100–1000 µm and temperatures in the range of 200–600 °C, and the substrate was divided into two layers, 2) a 220 µm thick middle layer, and 3) 3000 µm thick bottom layer as a substrate. The material of the middle layer and substrate was AZ31B, and it was assumed that the Mg and aluminum alloys did not mix during the coating. The middle layer was defined as a thin layer that would warm up very fast during the deposition of the coating material. The initial lengths of all three layers were equal (30 mm), and the initial temperature of the middle layer and substrate was set at 20 °C. However, the temperature of the top layer was changed, which will be explained for each case in the result section. In the first part of the simulation, the top and the middle layers were considered for modeling. In this situation, the length of the top layer and the middle layer was equal. The coating was set at a high temperature, while the middle layer was cold. After running the simulation, when the middle layer and substrate reached equilibrium, the residual stress was developed in these two layers due to the thermal mismatch between Mg and aluminum alloys. Then, the bottom layer (substrate) was added to the model. After adding the substrate, the residual stress in the three-layer system was calculated when the system was cooled to room temperature.

Table 3
CT scanning parameters.

Voxel size (μm)	Source-to-detector distance (mm)	Field of view (μm)	Voltage (kV)	Power (W)	Source filter Exposure time (s)	Optical magnification	Camera binning	Number of projections
3.5	35.064	3472.694	80	7	1	4.0021	2	2001

3. Results and discussion

3.1. Simulation results

The residual stresses induced in cold spray consist of mechanical stresses due to the peening effect and thermal stresses, particularly thermal mismatch between coating and substrate due to temperature effect. Experimentally, it is hard to dissociate these two effects from one another. Therefore, to better understand the thermal stresses in the dissimilar Aluminum/Magnesium sample, a finite element model was developed. This model only demonstrated the effect of temperature evolution during cooling of the coated part, while the stress induced by the peening effect was neglected. The preliminary results were extracted to reveal the impact of coating thickness on thermal stress distribution in the coating and substrate. For this, the maximum temperature was kept at 400 °C for the top layer (coating) and then reduced within the middle layer to 190 °C and reduced to room temperature of 20 °C for the substrate. Coating-layer thicknesses ranging from 100 μm to 500 μm were selected for this thermomechanical simulation. Fig. 1a shows the thermal stress distribution of the coated samples at the various coating thicknesses. Obvious discrepancies appear between the thermal stress of the coating and substrate, especially at the interface region. This finding can be attributed to the thermal expansion coefficient (CTE) differences of aluminum and Mg alloys. The CTE of aluminum alloy is less than that of Mg; hence, the thermal strain of aluminum alloy would be less than Mg alloy's when they experience similar temperature changes. Since they are bonded together, both are subjected to stress from each other depending on their mechanical properties and thickness. Because aluminum alloy coating experiences less dimensional change than Mg alloy does, the coating exerts tensile stress on the substrate, and the substrate imposes compressive stress on the coating during cooling. Fig. 1a also shows the magnitude of residual stress at the interface, revealing considerable changes from negative to positive ranges. With an increase in the thickness of the deposited layer, the slope of the residual stress curve in the coating area as well as the absolute value of thermal stress on the coating-free surface decrease, as a result of the bending stress distribution in the composite beam and thermal stress (see Fig. 1c). However, the thermal stress of the substrate surface near the interface underwent no significant changes when the coating thickness was changed (Fig. 1a).

Since coating tends to be more affected by thickness changes, its thermal stress of coated parts was investigated at different coating temperatures ranging from 200–600 °C. Fig. 1b shows the distribution of the stress through the coating thickness when the maximum coating temperature is increased to the specified temperatures. Thermal residual stress distribution in the coating is changed from a negative value to a positive one, with increasing the coating temperature or increasing the thickness at the constant temperature (see Fig. 1b). Therefore, the coating thickness and temperature have critical roles in inducing thermal stress in the substrate and coated parts. On the other hand, a minimum carrier gas temperature is required to feed the nozzle to accelerate the particles to supersonic velocity beyond the critical velocity and create bonding with the substrate. Nevertheless, the temperature of particles upon impact, and the deformation temperature, which is induced in a few nanoseconds, can still affect the residual stress of the substrate and overcome the peening effect.

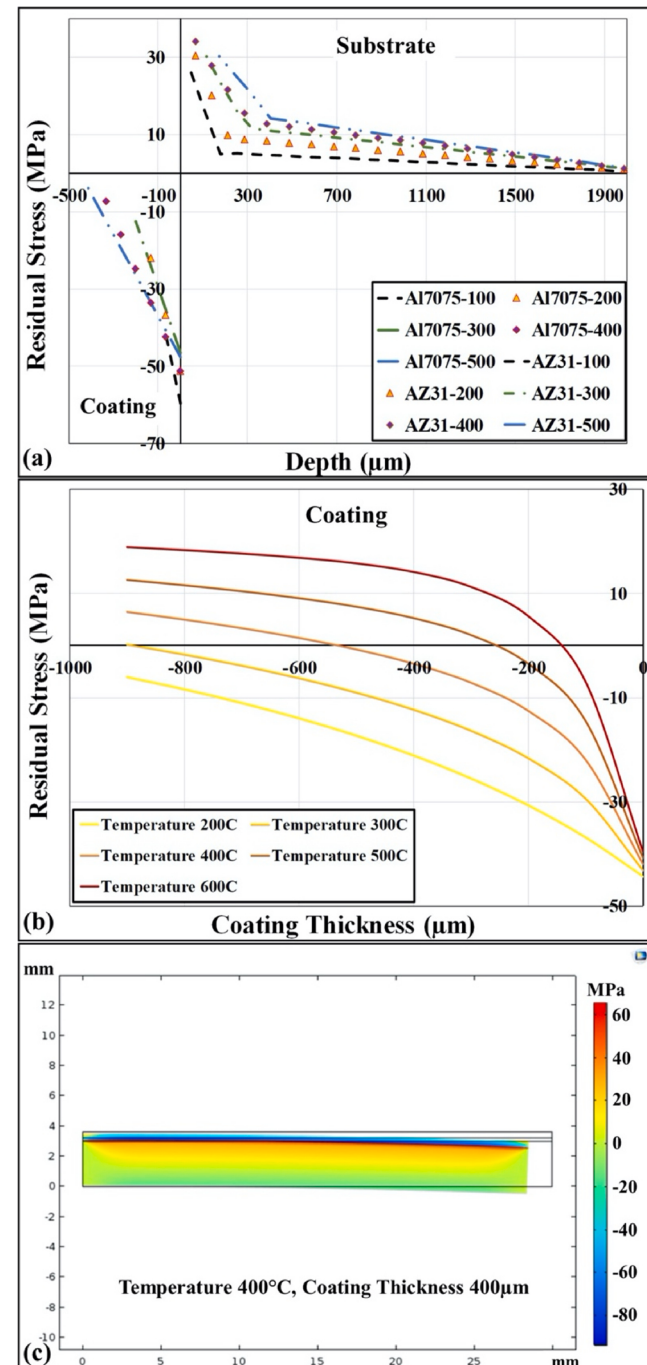


Fig. 1. a) Thermal stress distribution in coating with different thicknesses of 100–500 μm , and the substrate at the constant temperature of 400 °C; b) The stress distribution of the coated aluminum at different coating temperatures; c) An example of induced residual stress in the simulated part cooling down to room temperature.

3.2. Substrate temperature measurements

For better evaluation of the substrate temperature, temperature changes were monitored by the embedded thermocouple during the process (see Fig. 2a). The coating process was conducted for several samples in two different situations: with and without spraying powder (Fig. 2b). For all experiments, the carrier gas temperature and pressure were set at 400 °C and 1.38 MPa, respectively. Furthermore, different setups- with an insulated fixture and a fast cooling rate fixture (an aluminum plate) underneath the Mg substrate-were designed to study the effect of heat transfer during the coating process. First, the substrates were placed on the thermally insulated fixture, and the process was performed with and without powder deposition. The embedded thermocouple enabled the recording of the substrate's temperature 100 µm below the surface. It is well known that the basis for some of the existing theories of cold-spray bonding mechanisms is the local softening of particles and substrates due to the local heat induced by impact. However, because of the embedded thermocouple position, the measured temperature was far from the deformation temperature range, which is generated at a few hundreds of nanometers of the interface (Marzbanrad et al., 2018). Based on this observation and using the insulated fixture, the temperature was elevated to 190 °C when the nozzle was exactly over the thermocouple. Similar results were reported by Arabgol et al. (2014) when they measured the temperature of the substrate during the five-layer deposition of copper on copper and steel substrate. The recorded temperature was not more than 190 °C during the coating process, while the carrier gas temperature was 600 °C. Fig. 2c demonstrates no significant changes occurred between the temperature changes with and without depositing powder. These experiments were repeated several times, and the same results were observed. However, when an aluminum plate, with a much higher heat transfer rate than the former case, was situated under the substrate, there was about a 10 °C discrepancy between the two coating procedures (spraying carrier gas with and without powder). This observation can be explained by considering the heat transfer difference in the two cases. Using the insulated substrate, the temperature change between the hot top surface and cold bottom side of the substrate is less than in the other case. Therefore, the thermocouple recorded less difference where it was accommodated far from the substrate surface. Furthermore, in the aluminum fixture, the maximum temperature of the substrate reached 160 °C for the coating process, whereas this temperature was about 30 °C less than the maximum temperature of the substrate with the

insulated fixture. In addition, the cooling rate of the substrate with the aluminum fixture was considerably faster than that with the insulated fixture (see Fig. 2c). The most obvious finding to emerge from the temperature monitoring study is that the temperature of the substrate dropped by about 16 % when the aluminum fixture was replaced, with relatively good thermal conductivity.

3.3. Residual stress measurements

To examine the effect of temperature reduction on the residual stress formation in the cold spray coated samples, various experiments were carried out as listed in the studied variables column in Table 2. It is noted that the residual stress was measured on the stress relieved Mg alloy samples to disclose the residual stress resulting only from peening/hammering and thermal effects.

Fig. 3a shows the stress profiles of the coated samples under two different heat transfer boundary conditions: 1) fast cooling at the boundary and 2) insulated boundary condition at the constant and relatively low nozzle speed of 2 mm/s. These measurements show no substantial difference between the substrate residual stress, especially close to the interface. In contrast, the dissimilar trends of stress distribution in coated parts are greatly affected by the substrate fixtures (Fig. 3a). A considerable compressive residual stress value can be observed for the coated surfaces of samples when an Aluminum heatsink fixture was used to cool down the substrate compared with the other samples that were on the insulated fixture during the process. Moreover, the coating thickness of the samples placed on the Aluminum fixture is about 30 % less than that of the samples on the insulated fixture, despite the same processing parameters being used (see Fig. 3a). However, this temperature reduction due to accelerated heat conduction through the substrate could not affect the stress development in the substrate. The residual stress in the Mg sample at the interface is zero, although the compressive residual was expected in this region. This might be observed because the stress of the Mg substrate was relieved during the coating process. If this hypothesis is correct, for high-temperature sensitive materials like Mg, a greater temperature decrease is required to eliminate the impact of thermal energy on the properties of the sample. Since decreasing the carrier gas temperature, as a source of thermal energy, from the specified value of 400 °C leads to the decrease of the particle velocity, which will be lower than the critical velocity of the Al7075 particles, resulting in no or poor coating quality; hence, reduction of the exposure time by increasing the nozzle speed was considered.

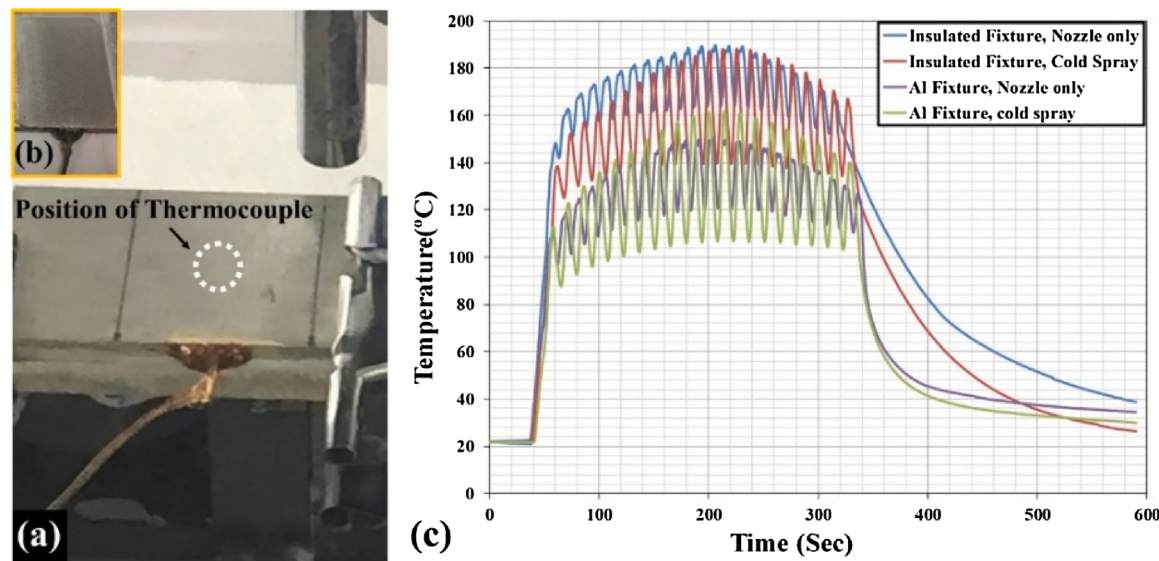


Fig. 2. a) The position of thermocouple after embedding into the Mg alloy substrate during the coating; b) Mg alloy sample with thermocouple; c) The temperature measurements of substrates fixed to an aluminum plate, and insulated during cold spray process.

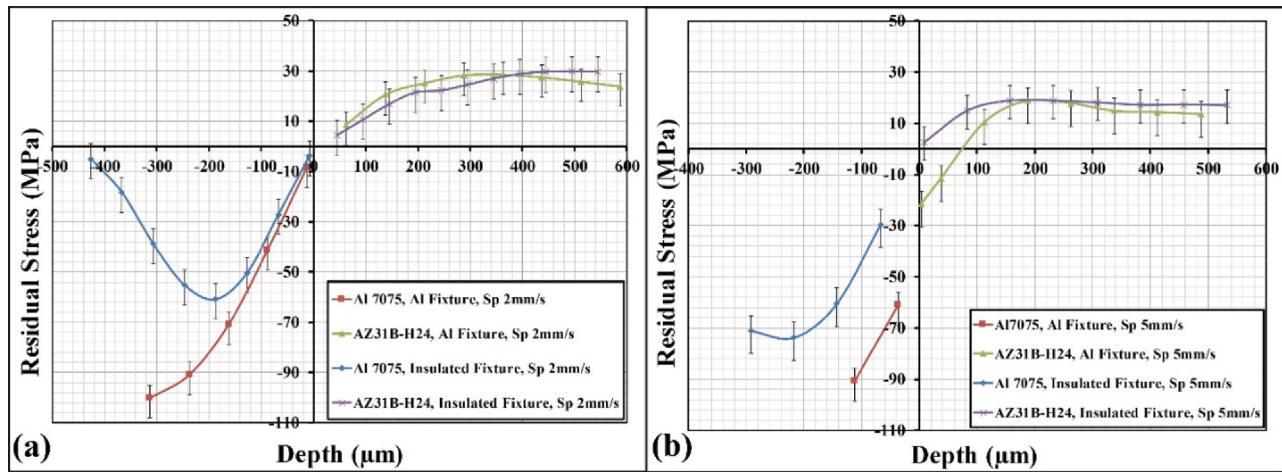


Fig. 3. Residual stress distributions for cold spray coated samples with different fixtures for placing the substrates, when the nozzle speed is a) 2 mm/s; and b) 5 mm/s.

Fig. 3b depicts the stress relaxation measurements for the coated samples with the nozzle speed of 5 mm/s for the two different fixtures. When nozzle speed is increased, improved surface residual stresses are formed in the coating for samples with the insulated fixture compare with the lower nozzle speed of 2 mm/s; whereas the residual stress in Mg substrates was relaxed similar to the samples treated with lower nozzle speed (**Fig. 3b**). However, For the samples that were situated on the Aluminum heatsink fixture and treated with 5 mm/s nozzle speed, the exposure time was not adequate to relieve the peening stress induced in the substrate; therefore, significant compressive residual stress was developed in the Mg substrate at the interface as well as the coated parts.

These tests showed that one can control the pattern of residual stress by controlling the acceleration of the heat transfer from the substrate and decreasing the heat input to the system. Heat transfer can be controlled by devising a proper cooling rate in the substrate, and heat input can be controlled by the nozzle speed. On the other hand, to compensate for the effect of reducing the temperature of the system during coating on the thickness of the deposited layer, feed rates need to be adjusted.

Building on this finding, experiments were designed to create a residual stress pattern that is compressive in both the coating and the substrate near the interface. For the rest of the study, the Aluminum heatsink was considered as a fixture under the Mg alloy substrates during the coating process to increase the cooling rate. Then, the effect of reducing the exposure time on the residual stress distribution in

coating and substrate was studied for various nozzle speeds from 2–20 mm/s, with two different feed rates of 25% (8 g/min) and 50% (16 g/min). **Fig. 4a** and **Fig. 4b** comparatively illustrate the residual stress distributions for different nozzle velocities at a constant feed rate low and high of 25% and 50%, respectively. However, the two combinations (feed rate = 25% and nozzle speed = 20 mm/s) and (feed rate = 50% and nozzle speed = 2 mm/s) were not considered, because in the former case, the coating thickness was too low to be utilized for the residual stress measurements. In the latter case, the deposited material was very thick, and the quality of the coating was not good enough to be considered for residual stress measurements. On the other hand, hole drilling reliable results are within 1 mm depth; hence, for measuring the residual stress through the thicker thickness another technique is required. Decreasing the coating thickness by increasing the nozzle speed inherently leads to reducing the number of particles impacting the surface. This trend can be observed in the results reported in **Fig. 4a** and b. By increasing the nozzle speed and, as a consequence, reducing the thermal input to the system, the compressive residual stress was enhanced in the coating as well as in the substrate materials at the interface. Moreover, the compressive residuals stress on the coating surface decreases in response to an increase of the coating thickness and decrease of the nozzle speed. This trend is observable for all cases except for the feed rate = 50% and nozzle speed = 20 mm/s. In this case, the peening was less effective because of the smaller number of impacting particles despite the higher feed rate. Therefore, the nozzle speed needs

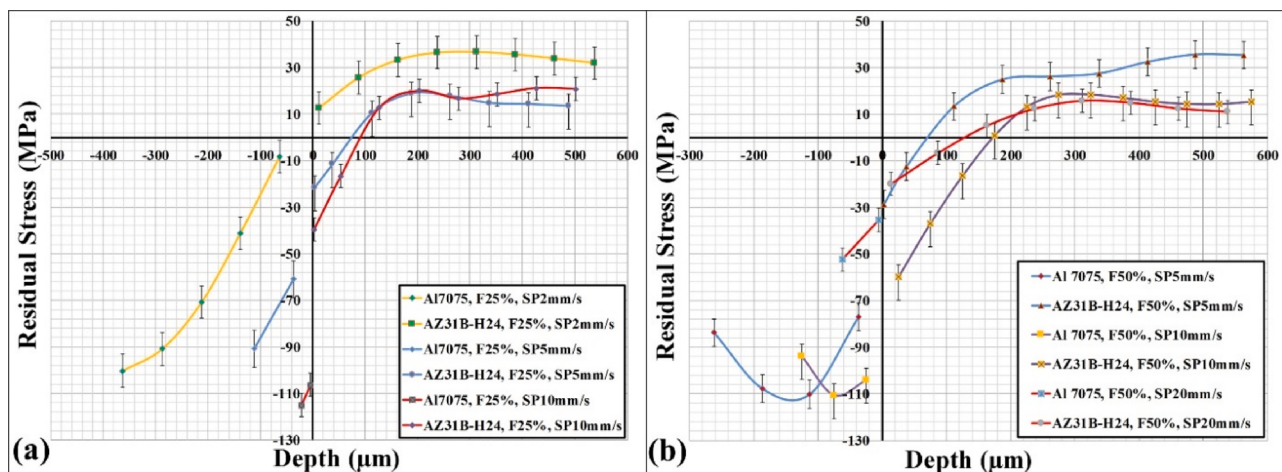


Fig. 4. Residual stress distributions for cold spray coated samples with different nozzle speed and feed rate; a) 25% (8gr/min); and b) 50% (16gr/min).

tight control to prevent negative effects on peening residual stress. In addition, comparing the effects of two feed rates with the same nozzle speed, increasing the feed rate means increasing the number of particles with effective impact, thereby increasing the beneficial residual stress due to the peening effect.

Another approach for achieving a specific coating thickness when the coating thickness is less than the expected value is to repeat the coating and let the sample cool down between the passes. To study the effect of temperature gradient in the multi-pass deposition approach on the residual stress induced in Mg and coated surfaces, the coating was performed for different samples at the constant processing parameters of feed rate = 50% nozzle speed = 20 mm/s. Fig. 5 shows through-the-depth residual stress distribution for different 1, 3, 5 passes. The residual stress was developed in a higher compressive amount at the substrate interface by increasing the number of passes as a result of an increasing number of impacts and improving the peening/hammering effect. However, the effect of thermal mismatching was predominant and reduced the compressive residual stress at the coating surface and even turned to the tensile for the 5 number of pass (Fig. 5). Therefore, even though increasing the number of passes promotes compressive residual stress at the interface, it can induce destructive tensile residual stress in the coated surface. The results confirm the simulation observations, especially for the coating surface with the high thickness, where the peening effect was influenced by the rising temperature and fast cooling for dissimilar materials, highlighting the thermal mismatch effect.

3.4. Effect of the coating parameters on the coating quality

The reported results in the previous sections revealed that the residual stress can be tailored to a desirable profile by controlling the nozzle travel speed, feed rate, and controlling the heat transfer from the substrate. Moreover, the results demonstrated that the coating thickness is changed when the residual stress is manipulated in the coating and substrate. Hence, it is expected that other characteristics of the coating will also change when the coating condition is modified. In the following sections, the surface quality, density, and mechanical properties of the coating have been investigated to highlight the effect of the proposed coating condition on the properties of the coating.

3.4.1. Surface morphology

To evaluate the effect of a coating's thickness on its surface roughness, coating thickness and surface roughness were measured for several coated samples, each treated with different process variables. Fig. 6a depicts the coating thickness and surface roughness for the samples coated with low and high feed rates of 25% and 50% and low and high

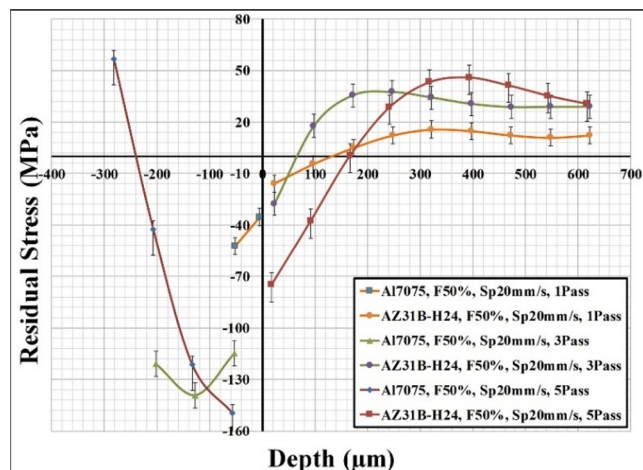


Fig. 5. Residual stress distributions of the cold spray coated samples with different numbers of passes.

nozzle speeds of 5 mm/s and 10 mm/s. The results show that the surface roughness increased by 24 % when the coating thickness was doubled. The same trend is also observed in -multi-pass experiments (Fig. 6b). Fig. 7 demonstrates the high-resolution topography images of two different coating surfaces with the minimum and maximum thicknesses among these experiments. In these figures, the maximum level of the peak for the samples with the lowest and highest surface roughness are shown. The minimum surface roughness of about 10.9 μm is obtained for the thinnest coating, and the maximum roughness of 22.7 μm belonged to the thickest coating in these series of experiments. (Tan et al., 2018) have reported the same observation of increasing surface roughness by increasing the coating thickness for cold sprayed Ti6Al4V coatings on Ti6Al4V substrates. To explain this observation, the authors argued that increasing the thickness raised the accumulation of heat generation during coating formation at the coating surface; hence, low-speed particles with a less than critical velocity have a chance to be partially deformed and attached to the surface as a result of the increased surface roughness. However, Fig. 7a and b show that the surfaces of both samples are covered with shallow indents with raised edges instead of hemispherical bumps, indicating partially deformed particles on the surface. This surface feature could represent the fingerprint of particles that impact the surface, are deformed, and joined to the coating. These observations can be explained by considering the heat generation during coating deposition. Thicker coating generates higher temperatures per unit time, and as a result, the particles are exposed to higher temperatures upon impact. Therefore, more softening, more deformation, and bigger indentations occur in the thicker coating materials during impact, as shown in Fig. 7b.

3.4.2. Computerized tomography (CT) analysis

The computerized tomography (CT) is utilized to investigate the integrity of the deposited material in the samples with tensile and compressive residual stress. The processing parameters for preparing the samples in these two extremes are listed in Table 4. The coating parameters to achieve the maximum compressive residual stress were assigned based on the minimum value of the surface roughness.

The CT scan results presented in Fig. 8 shows the quality of coating for the tensile and compressive samples. Based on the presented data, the pore density in the tensile sample was much greater than that in the compressive sample, and the pores were uniformly distributed throughout the cross-section of the sample (Fig. 8b). Fig. 9 depicts the pores size distribution of the tensile and compressive samples, and demonstrates that not only was the number of the pores in the tensile sample significantly more than that in the compressive sample but also that the average of the pore sizes was greater in the former than the latter. To address the exact densities of the coated samples, the equivalent solid fraction was calculated based on the pore and part voxels, which are listed in Table 5. It is concluded that 94% reduction of the porosity in compressive samples, representing the coating quality of the compressive samples was much better than that of the tensile ones. This observation contradicts results reported in the literature, claiming that increasing the temperature of the substrate improves the bond strength and the quality of coating (Watanabe et al., 2015). It is obvious that only a portion of the particles is accelerated to a specific velocity in the gas stream sufficient for successful impact and bonding, depending on their geometry and size. However, there is a chance for the other particles to sit on the surface, even partially deformed, and become trapped between the other particles, especially by the material jetting of their neighbors. Because of the trapped particles' geometry, the area around them is susceptible to pore formation. Moreover, increasing the temperature of the substrate provides more surface ductility, which promotes material jetting, and hence particles with low kinetic energy are trapped during unsuccessful impact. When the substrate is cold, it has higher yield strength; hence the substrate stores more elastic energy, which is released by the springing back effect, shooting the particle out. The strong spring back breaks the weak bond between the trapped particles

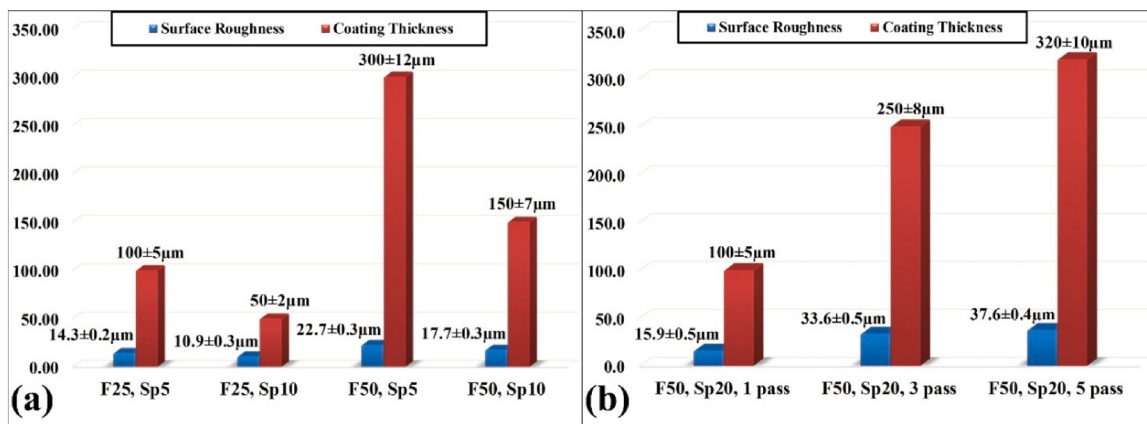


Fig. 6. Comparison between the coating thickness and the surface roughness of cold spray coated samples; a) for different feed rates and nozzle speeds; b) for different numbers of passes.

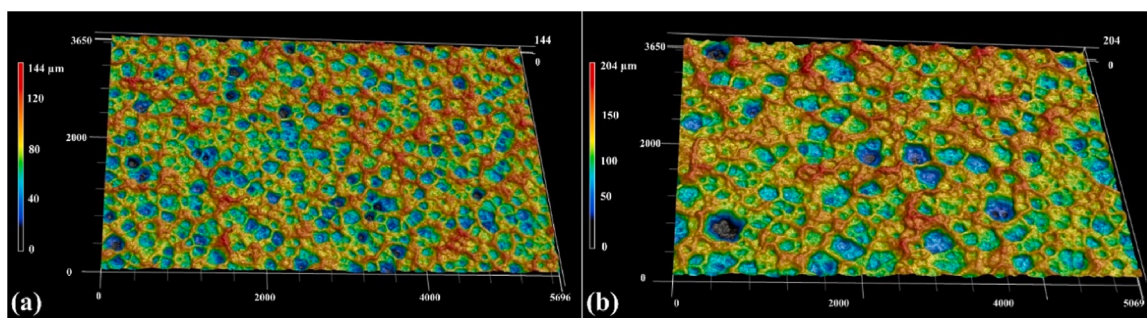


Fig. 7. Surface roughness images of coated samples with; a) $F = 25\%$ and $Sp = 10\text{ mm/s}$; b) $F = 50\%$ and $Sp = 5\text{ mm/s}$ (All dimensions are in μm).

Table 4

Processing parameters for inducing tensile and compressive residual stress in coated samples.

Coated Samples	Gas Temperature	Gas Pressure	Feed Rate	Nozzle Speed	Fixture
Tensile	400 °C	1.38 MPa	25% (8gr/min)	2 mm/s	Insulated
Compressive	400 °C	1.38 MPa	25% (8gr/min)	10 mm/s	Fast cooling rate

and the surface, thus releasing the particles. On the other hand, the coating efficiency is less for the cold substrate. In this case, in comparison with the higher temperature substrate at the constant feed rate, fewer particles consume their kinetic energy for deformation toward deposition. The rest of the particles have an elastic impact and help increase the density of the coating, and close the pores by hammering effect. Combinations of these effects work to increase the coating density when the substrate is kept cold.

3.4.3. Hardness analysis

Microhardness tests were conducted for the two types of coated samples: tensile and compressive samples. Fig. 10 shows that the microhardness of all AZ31B magnesium substrates is unchanged in the two samples and stays around 70 HV. However, the hardness of coating and interface differed. The compressive samples show an interface microhardness that is about 53% greater and a coating microhardness that is 13% greater than those of the tensile samples. Increase in the hardness may be due to two reasons: 1) compressive residual stress at the interface region and in the coating of compressive samples increases

the hardness due to limiting the indentation depth; 2) the compressive samples were kept cool, making the material less ductile and more work-hardened. Therefore, the peening effect is more effective in hardening the substrate and coating. A similar observation has been reported by Toshia (2002) where the effect of compressive residual stress induced by shot peening and bending on the hardness of carbon steel samples was examined. The hardness of the samples was increased when the compressive residual stress induced by shot peening and bending was enhanced.

4. Conclusions

The effect of substrate temperature and exposure time on residual stress formation in the coated Al7075 on AZ31B was investigated. By controlling the heat input (nozzle speed), cooling rate (substrate heat transfer), and the number of colliding particles (feed rate), desirable tensile and/or compressive residual stress were produced in the substrate near the interface and at the coating surface depending on the coating conditions and substrate temperature. The physical and mechanical properties and the quality of the coating were influenced by the coating parameters corresponding to these two types of residual stress. The results support the following conclusions:

- 1) Reducing the coating thermal energy by decreasing the exposure time and reducing the substrate temperature by using a heat sink to cool the substrate during coating can significantly influence the state of residual stress in the coated samples. For this, a nozzle speed of 10 mm/s was selected as an optimum velocity for inducing the compressive residual stress in the Mg substrate at the vicinity of the interface as well as in the coating surface.
- 2) By decreasing the nozzle speed to 5 or 2 mm/s and raising the substrate temperature by employing thermal insulation, the thermal

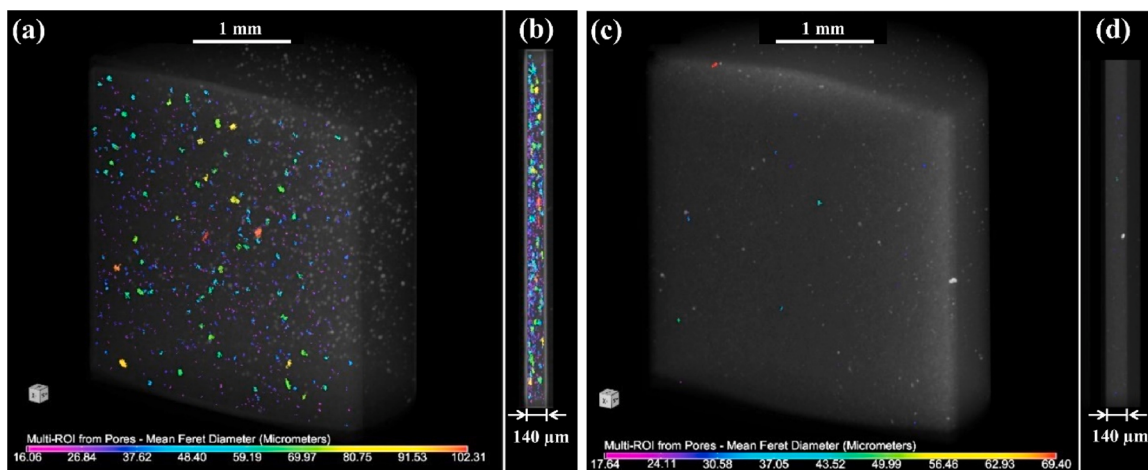


Fig. 8. Micro-scale tomography (CT) scanning: a) 3D image of the tensile coated sample; b) distribution of the pores in the coating thickness of the tensile sample; c) 3D image of the compressive sample; d) distribution of the pores in the coating thickness of the compressive sample.

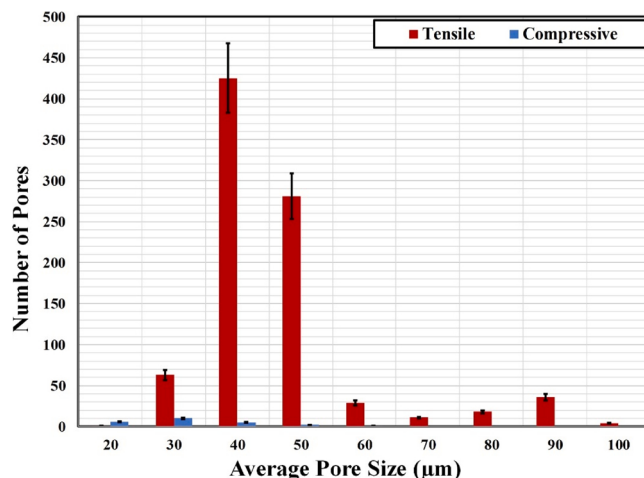


Fig. 9. Pores size population in the coating of the tensile and compressive samples.

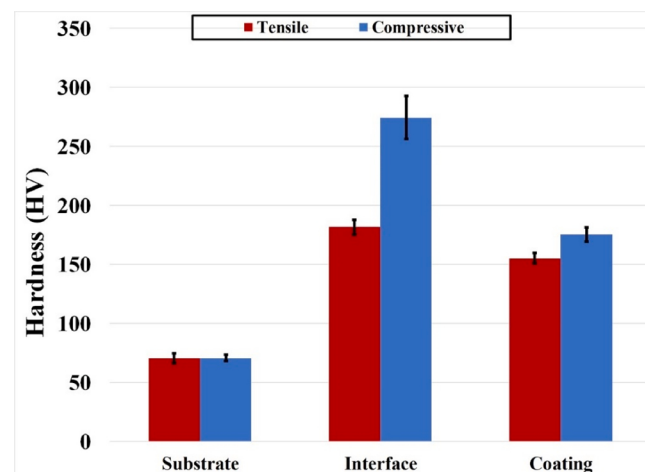


Fig. 10. Microhardness of the coated samples in three different regions (substrate, interface, and coating) for compressive residual stress and the samples with tensile residual stress at the substrate interface.

Table 5
The coating density of the tensile and compressive samples.

Coated Samples	Pore Voxels	Part Voxels	Equivalent Solid Fraction
Tensile	235,574	43,591,534	99.46%
Compressive	14,997	44,609,663	99.97%

- effect can overcome the peening effect, resulting in tensile residual stress in the substrate.
- 3) At a constant nozzle speed, increasing the feed rate (for example, from 25% to 50%) can manipulate the peening effect to impose beneficial compressive residual stresses in the coated samples. However, increasing the powder feed rate had less impact on increasing the coating temperature compared to the nozzle speed.
 - 4) Based on the simulation results, the thermal mismatch between the Al7075 coating and AZ31B substrate had a negative impact on the Mg substrate because of the tensile residual stress induced in the substrate. Reducing the coating temperature is essential to minimizing the detrimental effects of thermal mismatch. In addition, based on the results of this research, reducing the coating temperature and using a heat sink to cool the substrate during coating decreases coating surface roughness, which in turn reduces the risk of undesirable fatigue crack initiation at the interface.

- 5) A successful strategy for increasing coating thickness and maintaining compressive residual stresses in the substrate involves increasing the number of passes at a high nozzle speed. This approach maintains the compressive residual stress and even increases it due to the extra hammering effect. Similarly, increasing the powder feed rate and maintaining a constant nozzle speed leads to a higher coating thickness with the compressive residual stress.
- 6) The surface roughness was directly related to the coating thickness of the deposited layer. The powder impact indented the surface and produced the raised edges that the surface topography revealed to be the origin of surface roughness. This observation was justified by the coating and substrate temperature. The greater coating thickness increased the coating temperature, making the coated material softer, which promotes bigger indentations and higher impact edges.
- 7) The coating quality and the coating density of the compressive samples were higher than those of the tensile samples. Moreover, the size of pores in the compressive samples was smaller than those in the tensile samples.
- 8) Forming the coating at a lower coating temperature increased the hardness of the interface and coating.

CRediT authorship contribution statement

Bahareh Marzbanrad: Conceptualization, Data curation, Investigation, Methodology, Formal analysis, Writing - original draft. **Ehsan Toyserkani:** Conceptualization, Supervision, Methodology, Validation, Writing - review & editing. **Hamid Jahed:** Conceptualization, Methodology, Supervision, Funding acquisition, Writing - review & editing.

Declaration of Competing Interest

The authors report no declarations of interest.

Acknowledgments

The financial support of the Natural Sciences and Engineering Research Council of Canada (NSERC) through the Automotive Partnership Canada (APC) under APCPJ 459269-13, and NSERC-RTI program under EQPEQ458441-2014 grant is gratefully acknowledged.

Appendix A. Supplementary data

Supplementary material related to this article can be found, in the online version, at doi:<https://doi.org/10.1016/j.jmatprotec.2020.116928>.

References

- Arabgol, Z., Assadi, H., Schmidt, T., Gärtner, F., Klassen, T., 2014. Analysis of thermal history and residual stress in cold-sprayed coatings. *J. Therm. Spray Technol.* 23, 84–90. <https://doi.org/10.1007/s11666-013-9976-x>.
- Assadi, H., Gärtner, F., Stoltenhoff, T., Kreye, H., 2003. Bonding mechanism in cold gas spraying. *Acta Mater.* 51, 4379–4394. [https://doi.org/10.1016/S1359-6454\(03\)00274-X](https://doi.org/10.1016/S1359-6454(03)00274-X).
- Boruah, D., Ahmad, B., Lee, T.L., Kabra, S., Syed, A.K., McNutt, P., Doré, M., Zhang, X., 2019. Evaluation of residual stresses induced by cold spraying of Ti-6Al-4V on Ti-6Al-4V substrates. *Surf. Coatings Technol.* 374, 591–602. <https://doi.org/10.1016/j.surfcoat.2019.06.028>.
- Dayani, S.B., Shaha, S.K., Ghelichi, R., Wang, J.F., Jahed, H., 2018. The impact of AZ7075 cold spray coating on the fatigue life of AZ31B cast alloy. *Surf. Coatings Technol.* 337, 150–158. <https://doi.org/10.1016/j.surfcoat.2018.01.008>.
- Diab, M., Pang, X., Jahed, H., 2017. The effect of pure aluminum cold spray coating on corrosion and corrosion fatigue of magnesium (3% Al-1% Zn) extrusion. *Surf. Coatings Technol.* 309, 423–435. <https://doi.org/10.1016/j.surfcoat.2016.11.014>.
- Ghelichi, R., MacDonald, D., Bagherifard, S., Jahed, H., Guagliano, M., Jodoin, B., 2012. Microstructure and fatigue behavior of cold spray coated Al5052. *Acta Mater.* 60, 6555–6561. <https://doi.org/10.1016/j.actamat.2012.08.020>.
- Luzin, V., Spencer, K., Zhang, M.X., 2011. Residual stress and thermo-mechanical properties of cold spray metal coatings. *Acta Mater.* 59, 1259–1270. <https://doi.org/10.1016/j.actamat.2010.10.058>.
- Marzbanrad, B., Jahed, H., Toyserkani, E., 2018. On the evolution of substrate's residual stress during cold spray process: a parametric study. *Mater. Des.* 138, 90–102. <https://doi.org/10.1016/j.matdes.2017.10.062>.
- Matejicek, J., Sampath, S., 2001. Intrinsic residual stresses in single splats produced by thermal spray processes. *Acta Mater.* 49, 1993–1999. [https://doi.org/10.1016/S1359-6454\(01\)00099-4](https://doi.org/10.1016/S1359-6454(01)00099-4).
- Metal Handbook: 4E: Heat Treating of Nonferrous Alloys, 2018. Metal Handbook: 4E: Heat Treating of Nonferrous Alloys. ASM International.
- Salarian, M., Toyserkani, E., 2018. The use of nano-computed tomography (nano-CT) in non-destructive testing of metallic parts made by laser powder-bed fusion additive manufacturing. *Int. J. Adv. Manuf. Technol.* 98, 3147–3153. <https://doi.org/10.1007/s00170-018-2421-z>.
- Sampath, S., Jiang, X.Y., Matejicek, J., Prchlik, L., Kulkarni, A., Vaidya, A., 2004. Role of thermal spray processing method on the microstructure, residual stress and properties of coatings: an integrated study of Ni-5 wt. % Al bond coats. *Mater. Sci. Eng. A* 364, 216–231. <https://doi.org/10.1016/j.msea.2003.08.023>.
- Schajer, G.S., 1988. Measurement of non-uniform residual stresses using the hole-drilling method. Part ii—practical application of the integral method. *J. Eng. Mater. Technol.* 110, 344–349.
- Shayegan, G., Mahmoudi, H., Ghelichi, R., Villafuerte, J., Wang, J., Guagliano, M., Jahed, H., 2014. Residual stress induced by cold spray coating of magnesium AZ31B extrusion. *Mater. Des.* 60, 72–84. <https://doi.org/10.1016/j.matdes.2014.03.054>.
- Singh, R., Schrufer, S., Wilson, S., Gibmeier, J., Vassen, R., 2018. Influence of coating thickness on residual stress and adhesion-strength of cold-sprayed Inconel 718 coatings. *Surf. Coatings Technol.* 350, 64–73. <https://doi.org/10.1016/j.surfcoat.2018.06.080>.
- Song, X., Everaerts, J., Zhai, W., Zheng, H., Tan, A.W.Y., Sun, W., Li, F., Marinescu, I., Liu, E., Korsunsky, A.M., 2018. Residual stresses in single particle splat of metal cold spray process – numerical simulation and direct measurement. *Mater. Lett.* 230, 152–156. <https://doi.org/10.1016/j.matlet.2018.07.117>.
- Sova, A., Courbon, C., Valiorgue, F., Rech, J., Bertrand, P., 2017. Effect of turning and ball burnishing on the microstructure and residual stress distribution in stainless steel cold spray deposits. *J. Therm. Spray Technol.* 26, 1922–1934. <https://doi.org/10.1007/s11666-017-0655-1>.
- Suhonen, T., Varis, T., Dosta, S., Torrell, M., Guilemany, J.M., 2013. Residual stress development in cold sprayed Al, Cu and Ti coatings. *Acta Mater.* 61, 6329–6337. <https://doi.org/10.1016/j.actamat.2013.06.033>.
- Tan, A.W.Y., Sun, W., Bhowmik, A., Lek, J.Y., Marinescu, I., Li, F., Khun, N.W., Dong, Z., Liu, E., 2018. Effect of coating thickness on microstructure, mechanical properties and fracture behaviour of cold sprayed Ti6Al4V coatings on Ti6Al4V substrates. *Surf. Coatings Technol.* 349, 303–317. <https://doi.org/10.1016/j.surfcoat.2018.05.060>.
- TECHNOLOGY, E. (Ed.), 2014. EPO-TEK 353ND.
- Toscano, D., Shah, S.K., Behravesh, B., Jahed, H., Williams, B., 2017. Effect of forging on the low cycle fatigue behavior of cast AZ31B alloy. *Mater. Sci. Eng. A* 706, 342–356. <https://doi.org/10.1016/j.msea.2017.08.086>.
- Tosha, K., 2002. Influence of residual stresses on the hardness number in the affected layer produced by shot peening. Second Asia-Pacific Forum Precis. Surf. Finish. Deburring Technol. 48–54.
- Tsui, Y.C., Clyne, T.W., 1997. An analytical model for predicting residual stresses in progressively deposited coatings Part 1" Planar geometry. *Thin Solid Films* 306, 23–33.
- Wang, Q., Luo, X., Tsutsumi, S., Sasaki, T., Li, C., Ma, N., 2020. Measurement and analysis of cold spray residual stress using arbitrary Lagrangian-Eulerian method. *Addit. Manuf.* 35, 101296 <https://doi.org/10.1016/j.addma.2020.101296>.
- Watanabe, Y., Yoshida, C., Atsumi, K., Yamada, M., Fukumoto, M., 2015. Influence of substrate temperature on adhesion strength of cold-sprayed coatings. *J. Therm. Spray Technol.* 24, 86–91. <https://doi.org/10.1007/s11666-014-0165-3>.
- Xue, Y., Pang, X., Jiang, B., Jahed, H., 2019. Corrosion and corrosion fatigue performances of micro-arc oxidation coating on AZ31B cast magnesium alloy. *Mater. Corros.* 70, 268–280. <https://doi.org/10.1002/maco.201810293>.